JOURNAL OF AIRCRAFT
Vol. 47, No. 6, November–December 2010

Engineering Notes

Decay of Aircraft Wake Vortices Under Daytime Free Convective Conditions

Lakshmi Kantha*
University of Colorado, Boulder, Colorado 80309

DOI: 10.2514/1.C000322

Nomenclature

B	=	buoyancy flux, m^2/s^3
b	=	span, m
b_0	=	vortex spacing, m
g_0	=	gravitational acceleration, m/s^2
h	=	height above the ground, m
h_{ABL}	=	height of the atmospheric boundary layer, m
N	=	buoyancy frequency, $1/s$
Q	=	heat flux, W/m^2
Re	=	Reynolds number
s_0	=	characteristic distance scale, m
t, T	=	time, s
t_0	=	characteristic time scale, s
V_∞	=	aircraft speed, m/s
W	=	aircraft weight, N
w_0	=	characteristic velocity scale, m/s
β	=	safe nondimensional circulation, Γ_{safe}/Γ_0
Γ_0	=	circulation, m^2/s
ε	=	turbulence kinetic energy dissipation rate, m^2/s^3
ν	=	kinematic viscosity, m^2/s
ξ	=	nondimensional distance, s/s_0
Π	=	nondimensional circulation, Γ/Γ_0
τ	=	nondimensional time, t/t_0
Ω	=	atmospheric turbulence number, $b(\varepsilon b)^{1/3}/\Gamma_0$

Introduction

THE wake vortices generated by aircraft [1–3] are a severe hazard to other aircraft following behind. Because of mutual interaction, the trailing vortex pair descends at a rate of roughly 1.3 to 2.0 m/s for all but extremely light aircraft. Therefore, if the trailing aircraft stays well above the level of the leading aircraft, the chances of wake vortex encounter are small. Nevertheless, the rate of decay of these vortices is important to determining the allowable separation times and, hence, distances between aircraft during the landing approach; therefore, it is the principal factor in capacity limitation at busy airports. The International Civil Aviation Organization (ICAO) defines minimum separation distances, which have been rather conservative because of the paramount need for safety. Even a moderate easing of the separation standards would lead to a significant increase in airport capacities around the world. Given the fact that air travel is expected to double or even triple by 2025, and very few airports are being built at major metropolitan centers, increasing the throughput is perhaps the only solution to the projected increase in air traffic without causing undue inconvenience to the traveling public and undesirable environmental impact due to inevitable delays and airport congestion. Gerz et al. [4] presented current knowledge on transport and decay of wake vortices in the atmosphere and outlined concepts and designs of wake vortex advisory systems in Europe and the United States.

The desire to increase airport capacity has been the motivating factor behind the accelerated research, funded by federal agencies in Europe and the United States, into wake vortices [5–9] over the past decade. This has resulted in the development of capabilities to measure the intensity of wake vortices using advanced pulsed- and continuous-wave (CW) Doppler lidars [10–17] and other sensors [18–20]. These Doppler lidars can measure the vortex decay rates quite accurately. For a comparison of pulsed-wave and CW Doppler lidar measurements of wake vortices, see Kopp et al. [16] and Rahm et al. [17]. Dougherty et al. [19] described the deployment of a large passive acoustic microphone phased array at the Denver International Airport. The array was able to clearly resolve the wake vortices of landing aircraft and measure their separation, height, and sinking rate, provide visualization of the vortex evolution, including the Crow instability, and permit an indirect estimate of the vortex circulation. Burnham and Hallock [20] described the deployment of propeller anemometer arrays under the approach path at John F. Kennedy International Airport to study vortex transport and provide information about the vortex interaction with the ground. There has also been a concerted effort to model wake vortices [21–25]. Holzapfel [21] described a phenomenological probabilistic model for wake vortex decay, and Holzapfel et al. [22] conducted advanced numerical simulations of vortex decay in stably stratified atmosphere using large-eddy simulations (LES).

As a result of investment in advanced technologies, we are now able to measure wake vortices and their decay accurately [16]. The accelerated research over the past decade has shown conclusively that the rate of decay of wake vortices in the flight direction involves two phases, with a more rapid decay during the second phase, brought on by instabilities. The decay rate is also a strong function of the ambient atmospheric turbulence. For example, Kopp et al. [16] showed that wake vortices decay 1.8 times faster under moderate turbulence than under very weak turbulence. However, they did not provide possible parameterization of the effect of turbulence on vortex decay. To assure safety under all possible conditions, current ICAO separation distances correspond to very weak or zero ambient turbulence. But under daytime convective conditions, especially during summer, the ambient turbulence is strong enough to promote a much faster decay of wake vortices and hence permit smaller separation distances while maintaining safety. This Note describes a simple model to account for daytime convection on wake vortex decay.

Influence of Turbulence on Wake Vortex Decay

The vortex sheet at the trailing edge of a wing generating lift rolls up quickly into two counter-rotating vortices with circulation Γ_0 around each. Even with the inboard flaps fully deployed, the two resulting vortex pairs merge quickly into one. The two vortices of the vortex pair are separated by a distance equal to σb, where b is the wingspan and σ is the span factor, usually taken to be equal to $\pi/4$, even though this is appropriate only for elliptic lift distribution. Aircraft landing with inboard flaps deployed generate both tip vortices and flap-edge vortices, but this four-vortex system is very quickly transformed into a two-vortex system through merger of the flap-edge and tip vortices, so that it is usually adequate to regard the wake vortices generated by an aircraft under all conditions (cruise, landing, and takeoff) as belonging to the conventional Prandtl–Lancaster horseshoe vortex system. Under these conditions, the wake vortex characteristic velocity and time scales are

Received 18 February 2010; revision received 13 July 2010; accepted for publication 13 July 2010.

*Department of Aerospace Engineering Sciences.

$$w_0 = \frac{\Gamma_0}{2\pi b_0} = \frac{2\Gamma_0}{\pi^2 b}; \qquad t_0 = \frac{b_0}{w_0} = \frac{2\pi b_0^2}{\Gamma_0} = \frac{\pi^3}{8}\frac{b^2}{\Gamma_0} \tag{1}$$

where $b_0 = \frac{\pi}{4}b$ is the vortex spacing. It is possible to define the characteristic distance scale as $s_0 = V_\infty t_0$, where V_∞ is the aircraft speed. Note that the initial circulation is

$$\Gamma_0 = \frac{W}{\rho V_\infty b_0} = \frac{4}{\pi\rho V_\infty}\left(\frac{W}{b}\right) \tag{2}$$

where W is the weight of the aircraft. Γ_0 depends on the span loading, the aircraft speed and, of course, ambient density so that proper characterization of an aircraft in terms of its wake strength requires consideration of its span loading and not just its mass.

At any point in time t, the strength of the wake vortex is characterized by its circulation $\Gamma(t)$. The relevant parameters in wake vortex decay are

$$\Gamma, \quad \Gamma_0, \quad b, \quad t, \quad \varepsilon, \quad N, \quad \text{and} \quad \nu \tag{3}$$

where ε is the dissipation rate of turbulence kinetic energy (TKE, in m^2/s^3) that characterizes the level of ambient atmospheric turbulence, N is the buoyancy frequency (1/s) characterizing the density stratification in the atmosphere, and ν is the molecular kinematic viscosity (m^2/s). Note that it is possible to use TKE itself as indicative of the level of turbulence. However, aircraft-borne in situ sensors are needed to measure TKE, whereas it is possible to infer the TKE dissipation rate remotely along the flight path using Doppler radars. It is the standard practice in atmospheric turbulence research to use the TKE dissipation rate to characterize the level of turbulence. We therefore use ε in Eq. (3). These seven parameters lead to five nondimensional quantities:

$$\frac{\Gamma}{\Gamma_0}, \quad \frac{t}{t_0}, \quad N^* = Nt, \quad Re = \frac{\Gamma_0}{\nu} \quad \text{and} \quad \Omega = \frac{b(\varepsilon b)^{1/3}}{\Gamma_0} \tag{4}$$

so that

$$\frac{\Gamma}{\Gamma_0} = \text{fn}\left(\frac{t}{t_0}, N^*, Re, \Omega\right) \tag{5}$$

Note that Ω, as defined previously, is equivalent to $(\varepsilon b)^{1/3}/w_0$. The Reynolds number Re is usually high enough so that laminar viscosity is not important to vortex decay. Under stable stratification (for example, at night), N^* is important, but it is an imaginary quantity under unstable convective conditions and can be ignored. This means

$$\frac{\Gamma}{\Gamma_0} = \text{fn}\left(\frac{t}{t_0}, \Omega \text{ only}\right) \tag{6}$$

Vortex decay data should be presented in the form of a plot of $\Pi = \frac{\Gamma}{\Gamma_0}$ as a function of $\tau = \frac{t}{t_0}$ for various values of Ω. However, this is not always done [16], and so it is difficult to interpret wake vortex observational data from Doppler lidars.

For air traffic spacing purposes, it is important to know the time involved in the circulation of the vortices trailing behind the leading aircraft decaying to a certain value indicated by $\beta = \Gamma_{\text{safe}}/\Gamma_0$, the precise value of which depends on the following aircraft. The normalized characteristic time for this to happen, $\tau_d = \frac{t_d}{t_0}$, and the corresponding characteristic distance (or aircraft spacing), $\xi_d = \frac{s_d}{s_0}$, are functions of only the atmospheric turbulence number, Ω, which dictates the rate of wake vortex decay under ambient turbulence.

Kopp et al. [16] presented pulsed-wave and CW lidar wake vortex decay data in the form of a plot of normalized circulation Π as a function of normalized time but for various values of ε, corresponding to very weak ($0.5–2 \times 10^{-4}$ m^3/s^2), weak ($2–5\times 10^{-4}$ m^3/s^2), and moderate ($5–20 \times 10^{-4}$ m^3/s^2) turbulence, instead of Ω. Nevertheless, they concluded that the time scale τ_d for Π to decrease to 0.5 was 4.5, 3.5, and 2.5; therefore, it was 1.8 times faster for moderate turbulence compared with very weak turbulence. Since the ratio of ε for the two cases is roughly 10 and, therefore, the ratio of Ω is $\sqrt[3]{10}$, this suggests $\tau_d, \xi_d \sim \Omega^{-3/4}$, which would yield a decay time-scale ratio of $(10)^{1/4} = 1.78$, close to what Kopp et al. [16] found. We therefore take

$$\tau_d,\ \xi_d = \alpha\Omega^{-3/4} \tag{7}$$

where $\alpha = \alpha(\beta)$ is a universal function of β (the level of decay) and is equal to unity for $\beta = 0.5$. It is, however, important to point out that a lot more similar measurements under a wide variety of atmospheric conditions, along with relevant statistical measures, are essential to confirm this relationship.

Note that ε is used instead of TKE, because it does not depend on the averaging window when measuring turbulence. The only assumption needed is that the spatial scales are in the inertial subrange of the turbulence energy spectrum so that ε is scale independent.

Free Convective Conditions

During the day, the ground is heated by solar radiation and, in the absence of cloud cover, the heat flux Q from the ground can be well approximated by a half sinusoid:

$$Q_0 = Q_p \sin\left[\pi\left(\frac{T - T_{\text{sr}}}{T_{\text{ss}} - T_{\text{sr}}}\right)\right], \qquad (T_{\text{sr}} \le T \le T_{\text{ss}}) \tag{8}$$

where T_{ss} and T_{sr} are sunset and sunrise times, T is the local time, and Q_p is the peak heat flux, which depends on the season. During summer, Q_p can be as high as 1000 W/m^2. Cloud cover cuts down the value of Q_0, but this is a quantity readily measured by meteorological instruments. The heat flux is a function of height h above the ground and varies linearly from the ground to the top of the diurnal atmospheric boundary layer (ABL), h_{ABL}, so that

$$Q = Q_0\left(1 - 1.2\frac{h}{h_{\text{ABL}}}\right) \tag{9}$$

The ABL height increases during the day, from a few hundred meters at sunrise to as much as a few kilometers at sunset, the rate of increase depending on the heat flux and atmospheric stability [26]. Within tens of minutes after the sunset, the heat flux reverses and the ABL collapses to 100 m or so and grows slowly during the night, the rate depending on the prevailing wind shear. In any case, the daytime ABL height is readily determined by a lidar; therefore, the heat flux at any level in the boundary layer is readily determined.

The corresponding buoyancy flux $B = \overline{w'b'}$ is given by $B = Qg_0/\rho c_p\theta_0$, where $g_0 = 9.81$ m/s^2 is the gravitational acceleration, ρ is the air density (1.225 $kg\,m^{-3}$ at standard sea level conditions), c_p is the specific heat (1004 $J\,kg^{-1}\,K^{-1}$), and θ_0 is the reference temperature (300 K). Under free convection, the only source of turbulence is the buoyancy flux, and under quasi-steady-state conditions, therefore, the TKE dissipation rate is exactly equal to the buoyancy flux, so that

$$\varepsilon = \gamma Q \tag{10}$$

(with Q in W/m^2).

$$\gamma = 0.27 \times 10^{-4}$$

Note that the vortex decay time scale τ_d is

$$\tau_d = \tau_d^w\left(\frac{\Omega}{\Omega_w}\right)^{-3/4} = \tau_d^w\left(\frac{\varepsilon}{\varepsilon_w}\right)^{-1/4} \tag{11}$$

where τ_d^w is the decay time scale under weak turbulence conditions, which can be taken to correspond [16] to $\varepsilon = \varepsilon_w = 10^{-4}$ m^2/s^3 and can be readily determined if ε is known.

Within the surface layer, which extends to roughly 50–100 m, the heat flux Q can be taken as equal to Q_0. Thus, for summertime

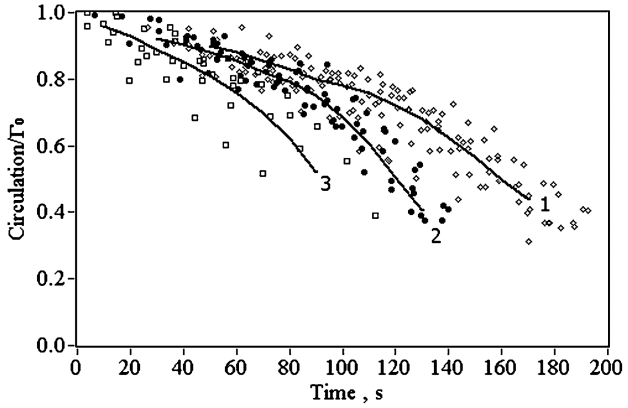

Fig. 1 Influence of atmospheric turbulence on behavior of normalized wake vortex circulation $\Pi = \Gamma/\Gamma_0$ at 1) $\varepsilon = 0.5 - 2 \times 10^{-4}$ m^2/s^3, 2) $\varepsilon = 2 - 5 \times 10^{-4}$ m^2/s^3, and 3) $\varepsilon = 5 - 2020 \times 10^{-4}$ m^2/s^3 (from [16]). Divide the time by 36 s to obtain normalized time $\tau = t/t_0$ (from Kopp et al. [16]).

conditions, the heat flux near the ground under cloud-free conditions during the day is of the order of 1000 W/m^2 at its peak; therefore, ε is 270×10^{-4} m^2/s^3. This means the wake vortex decay is four times faster than under weak turbulence conditions. Assuming the ABL height to be 2 km, even at a height of say 1 km above the ground, $Q = 400$ W/m^2, so that ε is 108×10^{-4} m^2/s^3, and the wake vortex decay is 1.8 times faster than under weak turbulence conditions. To be applicable to all atmospheric conditions, ICAO standard separation distances presume little to no ambient turbulence. Therefore, safe reductions in aircraft spacing might therefore be feasible and deserve to be investigated further.

More important, given the height of the aircraft within the ABL and the heat flux at the ground, the TKE dissipation rate ε can be readily determined from Eqs. (8) and (9) and, therefore, the enhanced vortex decay rate from Eq. (11). For $h/h_{\mathrm{ABL}} > 0.8$, it is probably safer to stick to ICAO separation distances.

It is not necessary to depend on the analytical results previously mentioned to determine the TKE dissipation rate in the atmosphere. Because of the technological advances in recent years, the dissipation rate in the ABL is readily measured by lidars [27,28], and the measured ε can be used in Eq. (11) to determine the safe spacing.

International Civil Aviation Organization Separations

Figure 1 shows observed wake vortex decay data from Kopp et al. [16], with $\Pi = \Gamma/\Gamma_0$ plotted against time in seconds (divide by 36 s to obtain normalized time $\tau = t/t_0$) for various atmospheric turbulence conditions. The two phases of wake vortex decay are clearly displayed at very weak turbulence conditions and can be described by a bilinear fit:

$$\Pi = 1 - 0.075[\Omega^{3/4}\tau], \quad [0 \le (\Omega^{3/4}\tau) \le 3.33]$$
$$= 0.75 - 0.225[(\Omega^{3/4}\tau) - 3.33], \quad [3.33 \le (\Omega^{3/4}\tau) \le 6.66] \quad (12)$$

These equations can be used to better understand the current ICAO separation distances, shown in Fig. 2. ICAO defines heavy as aircraft with a mass greater than 136,000 kg, and it defines medium as aircraft with a mass greater than 7000 kg but less than 136,000 kg. Light is defined as aircraft with mass less than 7000 kg. Since the heaviest aircraft (until the advent of the Airbus A-380) was Boeing 747-400, with a span of 64.4 m and a mass (at landing) of about 286,000 kg, Γ_0 is 648 m^2/s at 68.5 m/s (137 kt) and t_0 is 24.8 s. It was the worst possible heavy until the advent of the Airbus A380-800. Table 1 shows ICAO standards in terms of separation distances. Corresponding separation times assuming a cruise speed of 68.5 m/s (137 kt) are also shown. It is appropriate to remark here that time should be the basis of the separations between aircraft and not the distances per se, so that the influence of headwinds and tailwinds can be accounted for. Using Eq. (12), it is possible to determine the corresponding values of τ and Π, which are also shown. This enables the maximum possible Γ values encountered by the following aircraft to be determined, which are also shown.

The Boeing 757-200, with a mass of about 90,000 kg, a span of 38.1 m, a Γ_0 of 358 m^2/s, and a t_0 of 15.7 s, is taken as a typical medium aircraft. The Cessna Citation III, with a mass of 7000 kg, a span of 16.3 m, a Γ_0 of 64 m^2/s, and a t_0 of 16.1 s, is taken as the light aircraft. The corresponding values of τ and Π, and Γ, are also shown in Table 1.

For the Airbus A380-800, with a mass of 361,000 kg and a span of 79.8 m, Γ_0 is 673 m^2/s, roughly the same as the Boeing 747-400. However, t_0 is 36.7 s; hence, the separation times and distances have to be increased by roughly 50% compared with the 747. The bottom row of Table 1 shows these values.

From Table 1, it appears that the following aircraft can be considered safe if it encounters a wake vortex from the leading

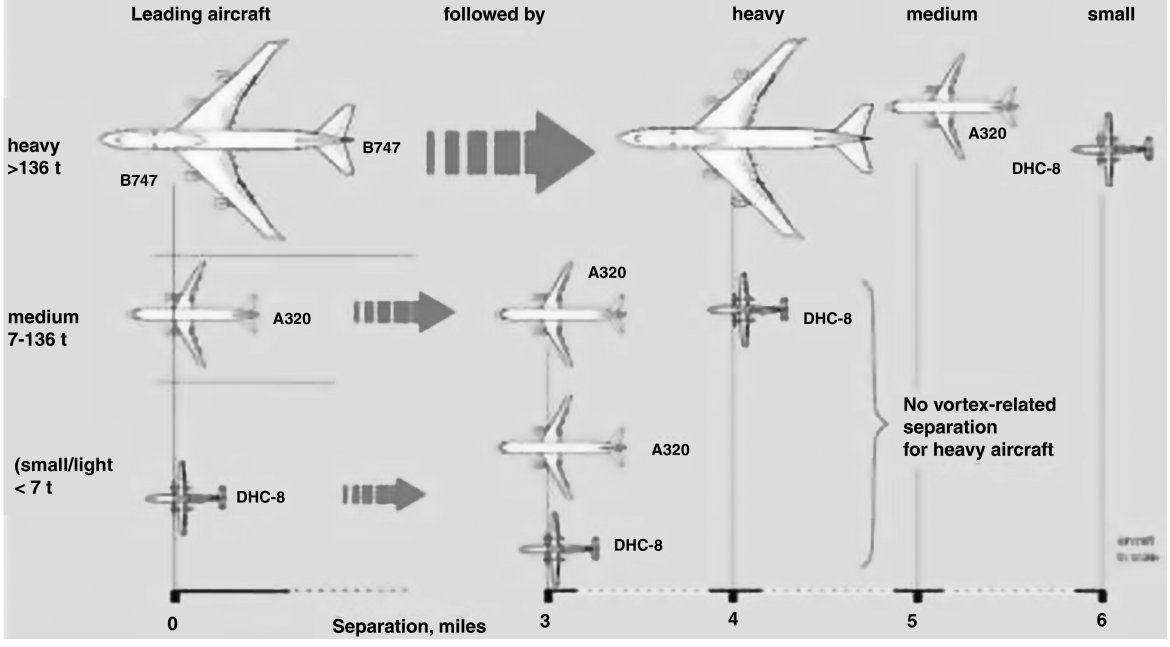

Fig. 2 Current ICAO separation distances.

Table 1 Current ICAO separations (top three rows)[a]

	Follower		
Leader	Heavy	Medium	Light
Heavy (>136, 000 kg)	4 NM ($t = 105$ s)	5 NM ($t = 131$ s)	6 NM ($t = 158$ s)
(B747-400: $t_0 = 24.3$ s)	$\tau = 4.3$, $\Pi = 0.53$	$\tau = 5.4$, $\Pi = 0.29$	$\tau = 6.5$, $\Pi = 0.04$
$\Gamma_0 = 661$ m^2/s	$\Gamma \leq 348$ m^2/s	$\Gamma \leq 189$ m^2/s	$\Gamma \leq 24$ m^2/s
Medium (<136, 000 kg)	——	3 NM ($t = 79$ s)	4 NM ($t = 105$ s)
(B757-200: $t_0 = 15.7$ s)	——	$\tau = 5.0$, $\Pi = 0.37$	$\tau = 6.7$, $\Pi = 0$
$\Gamma_0 = 351$ m^2/s	$\Gamma \leq 348$ m^2/s	$\Gamma \leq 129$ m^2/s	$\Gamma = 0$ m^2/s
Light (<7.000 kg)	——	——	3 NM ($t = 79$ s)
(Citation III: $t_0 = 16.1$ s)	——	——	$\tau = 4.9$, $\Pi = 0.4$
$\Gamma_0 = 64$ m^2/s	$\Gamma \leq 348$ m^2/s	$\Gamma \leq 129$ m^2/s	$\Gamma \leq 24$ m^2/s
Heavy (A380-800)	6.1 NM ($t = 160$ s)	7.6 NM ($t = 199$ s)	9.1 NM ($t = 234$ s)
($\Gamma_0 = 673$ m^2/s, $t_0 = 36.7$ s)	$\tau = 4.4$, $\Pi = 0.52$	$\tau = 5.4$, $\Pi = 0.28$	$\tau = 6.5$, $\Pi = 0.04$
	$\Gamma \leq 348$ m^2/s	$\Gamma \leq 189$ m^2/s	$\Gamma \leq 24$ m^2/s

[a]These values are to be taken as corresponding to very weak turbulence conditions. What happens when the leading heavy is replaced by the A380-800 is shown in the bottom (fourth) row.

aircraft with a maximum Γ less than roughly half its own Γ_0. Since Γ_0 is proportional to the span lading W/b, this means that the separation time (distance) has to be such that

$$\Pi \leq \beta \left(= \frac{\Gamma_0^F}{2\Gamma_0^L} = \frac{1}{2}\frac{(W/b)^F}{(W/b)^L} \right)$$

This is easily determined for various aircraft combinations. It also suggests that the aircraft span loading is more relevant to aircraft separations than the weight of the aircraft per se. Table 2 provides the relevant wake vortex parameters for a few selected transport aircraft. Table 3 provides the separation times and distances for a combination of the A380-800 (very heavy), the B747-400 (heavy), the B777-200 (medium), the B787-8 (light medium), the B757-200 (light), the B737 (very light), the Cessna Citation II (ultralight), and the Cessna 150M (ultra ultralight) based on Eq. (12). Clearly, for some combinations, it may be feasible to reduce separation times (and hence distances) to the minimum governed by considerations other than wake vortex hazard. Note that the criterion selected to determine the values in Table 3 is not unique, but the separation times and distances are easily determined from Eq. (12) for any other assumption about the appropriate value of β.

Conclusions

Observations over the past decade show that wake vortices can persist [16,29] as long as 160 s, while they are also known to decay rapidly in as little as 40 s. This is a ratio of four and corresponds well to the absolute theoretical maximum enhancement in the wake vortex decay rate for a given aircraft of around four, mentioned previously. In practice, to err on the safer side, the maximum enhancement should probably be taken to be around two under strong convective conditions, i.e., corresponding to strong summertime diurnal peak in solar heating. The wind does somewhat enhance the turbulence levels in the ABL. However, this enhancement can be neglected without much error. It is also reasonable to assume no enhancement in the vortex decay rate for a few hours around sunrise and sunset, and during the night. In fact, during the night, turbulence can be completely suppressed by stable stratification in the shallow nocturnal ABL, especially under windless conditions. These conditions are then ideal for wake vortices to linger or be transported to adjacent runways, but abundant experience over the past few decades suggests that the current ICAO separations appear to suffice for safe operations under these conditions.

The study suggests that separation times can be prudently lowered based on actual measured values of ε. Doppler lidars may therefore play a critical role in enhancing the handling capacity of busy airports

Table 2 Parameters relevant to wake vortices for selected civilian transport aircraft under takeoff, cruise, and landing conditions

	Aircraft	Mass, kg	b, m	W/b, N/m	AR	V_∞, m/s	Γ_0, m^2/s	w_0, m/s	t_0, s
Takeoff	A380-800	560,000	79.8(83)	68,842	7.5	97.6	712.0	1.74	37.5
	B747-400	396,900	64.4	60,459	7.7	97.3	633.3	1.99	25.4
	B777-200	263,080	60.9	42,378	8.7	88.4	508.1	1.69	28.3
	A330-200	230,000	60.3(62.7)	37,418	10.0	82.3	458.9	1.48	33.2
	B757-200	108,800	38.1	28,014	8.0	80.0	371.3	1.97	15.2
	A320-200	73,500	33.8(35.2)	21,332	9.5	74.0	290.9	1.67	16.5
Cruise	A380-800	460,500	79.8(83)	56,610	7.5	246	762.4	1.86	35.0
	B747-400	320,200	64.4	48,776	7.7	251	639.4	2.01	25.1
	B777-200	231,330	60.9	37,263	8.7	248	514.2	1.71	28.0
	A330-200	205,010	60.3(62.7)	33,352	10.0	242	449.1	1.45	33.9
	B757-200	96,200	38.1	24,770	8.0	242	350.3	1.86	16.1
	A320-200	67,500	33.8(35.2)	19,591	9.5	236	270.5	1.56	17.7
Landing	A380-800	361,000	79.8(83)	44,379	7.5	76.2	587.9	1.44	45.4
	B747-400	285,800	64.4	43,536	7.7	80.0	554.6	1.75	29.0
	B777-200	213,190	60.9	34,341	8.7	71.1	512.0	1.70	28.1
	A330-200	181,980	60.3(62.7)	29,606	10.0	72.6	411.6	1.33	37.0
	B787-8	172,000	57.9	29,142	9.2	70.0	424.1	1.48	30.6
	B757-200	89,800	38.1	23,122	8.0	67.0	365.8	1.95	15.4
	A320-200	64,500	33.8(35.2)	18,720	9.5	66.8	282.8	1.63	16.9
	B737-500	49,900	28.9	16,350	7.9	67.0	253.6	1.71	13.8
	Citation III	7,000	16.3	4,213	9.2	67.0	64.0	0.80	16.1
	Cessna 150M	730	10.2	702	6.9	40.0	18.2	0.36	22.1

Table 3 Separation times and distances at 137 kt (70.5 m/s) for various combinations of aircraft under very weak turbulence conditions determined by the condition that the circulation of the trailing vortices from the leading aircraft decay to a value equal to half that of the circulation of the following aircraft[a]

	Follower							
Leader	Very heavy	Heavy	Medium	Light medium	Light	Very light	Ultralight	Ultra ultralight
Very heavy (A380-800)	163 s, 6.2 NM	164 s, 6.3 NM	181 s, 6.9 NM	191 s, 7.3 NM	202 s, 7.7 NM	213 s, 8.1 NM	236 s, 9.0 NM	243 s, 9.3 NM
$\Gamma_0 = 673$ m^2/s	$\Gamma \leq 336$ m^2/s	$\Gamma \leq 330$ m^2/s	$\Gamma \leq 260$ m^2/s	$\Gamma \leq 221$ m^2/s	$\Gamma \leq 175$ m^2/s	$\Gamma \leq 129$ m^2/s	$\Gamma \leq 32$ m^2/s	$\Gamma \leq 5$ m^2/s
361,000 kg, $t_0 = 36.7$ s, $w_0 = 1.71$ m/s	$\Pi = 0.5$, $\tau = 4.4$	$\Pi = 0.5$, $\tau = 4.5$	$\Pi = 0.39$, $\tau = 4.9$	$\Pi = 0.33$,$\tau = 5.2$	$\Pi = 0.26$, $\tau = 5.5$	$\Pi = 0.19$, $\tau = 5.8$	$\Pi = 0.05$, $\tau = 6.5$	$\Pi = 0.05$, $\tau = 6.6$
Heavy (B747-400)	107 s, 4.1 NM	108 s, 4.1 NM	119 s, 4.6 NM	126 s, 4.8 NM	133 s, 5.1 NM	141 s, 5.4 NM	157 s, 6 NM	161 s, 6.1 NM
$\Gamma_0 = 661$ m^2/s	$\Gamma \leq 336$ m^2/s	$\Gamma \leq 330$ m^2/s	$\Gamma \leq 260$ m^2/s	$\Gamma \leq 221$ m^2/s	$\Gamma \leq 175$ m^2/s	$\Gamma \leq 129$ m^2/s	$\Gamma \leq 32$ m^2/s	$\Gamma \leq 5$ m^2/s
285,800 kg, $t_0 = 24.3$ s, $w_0 = 2.08$ m/s	$\Pi = 0.51$, $\tau = 4.4$	$\Pi = 0.5$, $\tau = 4.4$	$\Pi = 0.39$, $\tau = 4.9$	$\Pi = 0.33$, $\tau = 5.2$	$\Pi = 0.27$, $\tau = 5.5$	$\Pi = 0.19$, $\tau = 5.8$	$\Pi = 0.05$, $\tau = 6.4$	$\Pi = 0.01$, $\tau = 6.6$
Medium (B777-200)	105 s, 4 NM	106 s, 4.1 NM	123 s, 4.7 NM	132 s, 5 NM	143 s, 5.4 NM	154 s, 5.9 NM	176 s, 6.7 NM	183 s, 7 NM
$\Gamma_0 = 521$ m^2/s	$\Gamma \leq 336$ m^2/s	$\Gamma \leq 330$ m^2/s	$\Gamma \leq 260$ m^2/s	$\Gamma \leq 221$ m^2/s	$\Gamma \leq 175$ m^2/s	$\Gamma \leq 129$ m^2/s	$\Gamma \leq 32$ m^2/s	$\Gamma \leq 5$ m^2/s
213,190 kg, $t_0 = 27.6$ s, $w_0 = 1.73$ m/s	$\Pi = 0.65$, $\tau = 3.8$	$\Pi = 0.63$, $\tau = 3.8$	$\Pi = 0.5$, $\tau = 4.4$	$\Pi = 0.42$, $\tau = 4.8$	$\Pi = 0.34$, $\tau = 5.2$	$\Pi = 0.25$, $\tau = 5.6$	$\Pi = 0.06$, $\tau = 6.4$	$\Pi = 0.01$, $\tau = 6.6$
Light medium (B787-8)	93 s, 3.6 NM	98 s, 3.7 NM	119 s, 4.5 NM	130 s, 5 NM	144 s, 5.5 NM	158 s, 6 NM	186 s. 7.1 NM	194 s, 7.4 NM
$\Gamma_0 = 442$ m^2/s	$\Gamma \leq 336$ m^2/s	$\Gamma \leq 330$ m^2/s	$\Gamma \leq 260$ m^2/s	$\Gamma \leq 221$ m^2/s	$\Gamma \leq 175$ m^2/s	$\Gamma \leq 129$ m^2/s	$\Gamma \leq 32$ m^2/s	$\Gamma \leq 5$ m^2/s
172,000 kg, $t_0 = 29.4$ s, $w_0 = 1.55$ m/s	$\Pi = 0.76$, $\tau = 3.2$	$\Pi = 0.75$, $\tau = 3.3$	$\Pi = 0.59$, $\tau = 4.0$	$\Pi = 0.5$, $\tau = 4.4$	$\Pi = 0.40$, $\tau = 4.9$	$\Pi = 0.29$, $\tau = 5.3$	$\Pi = 0.07$, $\tau = 6.3$	$\Pi = 0.01$, $\tau = 6.6$
Light (B757-200)	9 s, 0.3 NM	13 s, 0.5 NM	54 s, 2.1 NM	62 s, 2.4 NM	71 s, 2.7 NM	81 s, 3.1 NM	100 s, 3.8 NM	106 s, 4 NM
$\Gamma_0 = 351$ m^2/s	$\Gamma \leq 336$ m^2/s	$\Gamma \leq 330$ m^2/s	$\Gamma \leq 260$ m^2/s	$\Gamma \leq 221$ m^2/s	$\Gamma \leq 175$ m^2/s	$\Gamma \leq 129$ m^2/s	$\Gamma \leq 32$ m^2/s	$\Gamma \leq 5$ m^2/s
89,800 kg, $t_0 = 16.0$ s, $w_0 = 1.87$ m/s	$\Pi = 0.96$, $\tau = 0.5$	$\Pi = 0.94$, $\tau = 0.8$	$\Pi = 0.74$, $\tau = 3.4$	$\Pi = 0.63$, $\tau = 3.9$	$\Pi = 0.50$, $\tau = 4.4$	$\Pi = 0.37$, $\tau = 5.0$	$\Pi = 0.09$, $\tau = 6.3$	$\Pi = 0.02$, $\tau = 6.6$
Very light (B737-500)	——	——	——	23 s, 0.9 NM	46 s, 1.7 NM	56 s, 2.1 NM	77 s, 2.9 NM	83 s, 3.2 NM
$\Gamma_0 = 257$ m^2/s	$\Gamma \leq 336$ m^2/s	$\Gamma \leq 330$ m^2/s	$\Gamma \leq 260$ m^2/s	$\Gamma \leq 221$ m^2/s	$\Gamma \leq 175$ m^2/s	$\Gamma \leq 129$ m^2/s	$\Gamma \leq 32$ m^2/s	$\Gamma \leq 5$ m^2/s
49,900 kg, $t_0 = 12.6$ s, $w_0 = 1.80$ m/s	——	——	——	$\Pi = 0.86$, $\tau = 1.9$	$\Pi = 0.68$, $\tau = 3.6$	$\Pi = 0.50$, $\tau = 4.4$	$\Pi = 0.12$, $\tau = 6.1$	$\Pi = 0.02$, $\tau = 6.6$
Ultralight (CS-CIII)	——	——	——	——	——	——	72 s, 2.7 NM	101 s, 3.9 NM
$\Gamma_0 = 63.9$ m^2/s	$\Gamma \leq 336$ m^2/s	$\Gamma \leq 330$ m^2/s	$\Gamma \leq 260$ m^2/s	$\Gamma \leq 221$ m^2/s	$\Gamma \leq 175$ m^2/s	$\Gamma \leq 129$ m^2/s	$\Gamma \leq 32$ m^2/s	$\Gamma \leq 5$ m^2/s
7,000 kg, $t_0 = 16.1$ s, $w_0 = 0.79$ m/s	——	——	——	——	——	——	$\Pi = 0.50$, $\tau = 4.4$	$\Pi = 0.08$, $\tau = 6.3$
Ultra ultralight (CS-150M)	——	——	——	——	——	——	——	——
$\Gamma_0 = 10.7$ m^2/s	$\Gamma \leq 336$ m^2/s	$\Gamma \leq 330$ m^2/s	$\Gamma \leq 260$ m^2/s	$\Gamma \leq 221$ m^2/s	$\Gamma \leq 175$ m^2/s	$\Gamma \leq 129$ m^2/s	$\Gamma \leq 32$ m^2/s	$\Gamma \leq 5$ m^2/s
730 kg, $t_0 = 37.9$ s, $w_0 = 0.21$ m/s	——	——	——	——	——	——	——	——

[a]Under moderate turbulence, multiply these values by a factor of 0.56. The separation values are easily determined for any other criterion.

around the world, since they provide the capability to remotely measure ε all along the flight corridor. Strong daytime convective conditions are often associated with good visibility; hence, visual flight rules prevail, and separation distances are reduced upon request by the pilots. However, the separation distances (times) could also be reduced under poor visibility and instrument flight rules, in particular, category 1 conditions.

References

[1] Rossow, V. J., "Lift-Generated Vortex Wakes of Subsonic Transport Aircraft," *Progress in Aerospace Sciences*, Vol. 35, No. 6, 1999, pp. 507–660.
doi:10.1016/S0376-0421(99)00006-8

[2] Gerz, T., Holzapfel, F., and Darracq, D., "Commercial Aircraft Wake Vortices," *Progress in Aerospace Sciences*, Vol. 38, No. 3, 2002, pp. 181–208.
doi:10.1016/S0376-0421(02)00004-0

[3] Jacquin, L., "Aircraft Trailing Vortices: an Introduction," *Comptes Rendus Physique*, Vol. 6, Nos. 4–5, 2005, pp. 395–398.
doi:10.1016/j.crhy.2005.06.001

[4] Gerz, T., Holzapfel, F., Bryant, W., Kopp, F., Frech, M., Tafferner, A., and Winckelmans, G., "Research Towards Wake-Vortex Advisory System for Optimal Aircraft Spacing," *Comptes Rendus Physique*, Vol. 6, Nos. 4–5, 2005, pp. 501–523.
doi:10.1016/j.crhy.2005.06.002

[5] Jacquin, L., Fabre, D., Sipp, D., and Coustols, E., "Unsteadiness, Instability and Turbulence in Trailing Vortices," *Comptes Rendus Physique*, Vol. 6, Nos. 4–5, 2005, pp. 399–414.
doi:10.1016/j.crhy.2005.05.007

[6] Meunier, P., Le Dizes, S., and Leweke, T., "Physics of Vortex Merging," *Comptes Rendus Physique*, Vol. 6, Nos. 4–5, 2005, pp. 431–450.
doi:10.1016/j.crhy.2005.06.003

[7] Paoli, R., and Garnier, F., "Interaction of Exhaust Jets and Aircraft Wake Vortices: Small-Scale Dynamics and Potential Microphysical-Chemical Transformations," *Comptes Rendus Physique*, Vol. 6, Nos. 4–5, 2005, pp. 525–547.
doi:10.1016/j.crhy.2005.05.003

[8] Savas, O., "Experimental Investigations on Wake Vortices and Their Alleviation," *Comptes Rendus Physique*, Vol. 6, Nos. 4–5, 2005, pp. 415–429.
doi:10.1016/j.crhy.2005.05.004

[9] Holzapfel, F., Hofbauer, T., Darracq, D., Moet, H., Garnier, F., and Ferreira Gago, C., "Analysis of Wake Vortex Decay Mechanisms in the Atmosphere," *Aerospace Science and Technology*, Vol. 7, No. 4, 2003, pp. 263–275.
doi:10.1016/S1270-9638(03)00026-9

[10] Vaughan, J. M., and Harris, M., "Lidar Measurement of B747 Wakes: Observation of a Vortex Within a Vortex," *Aerospace Science and Technology*, Vol. 5, No. 6, 2001, pp. 409–411.
doi:10.1016/S1270-9638(01)01115-4

[11] Harris, M., Young, R. I., Kopp, F., Dolfi, A., and Cariou, J.-P., "Wake Vortex Detection and Monitoring," *Aerospace Science and Technology*, Vol. 6, No. 5, 2002, pp. 325–331.
doi:10.1016/S1270-9638(02)01171-9

[12] Keane, M., Buckton, D., Redfern, M., Bollig, C., Wedekind, C., Kopp, F., and Berni, F., "Axial Detection of AircraftWake Vortices Using Doppler Lidar," *Journal of Aircraft*, Vol. 39, No. 5, 2002, pp. 850–861.
doi:10.2514/2.3005

[13] Kopp, F., Smalikho, I., Rahm, S., Dolfi, A., Cariou, J.-P., Harris, M., Young, R. I., Weekes, K., and Gordon, N., "Characterization of Aircraft Wake Vortices by Multiple-Lidar Triangulation," *AIAA Journal*, Vol. 41, No. 6, 2003, pp. 1081–1088.
doi:10.2514/2.2048

[14] Holzapfel, F., Gerz, T., Kopp, F., Stumpf, E., Harris, M., Young, R. I., and Dolfi, A., "Strategies for Circulation Evaluation of Aircraft Wake Vortices Measured by Lidar," *Journal of Atmospheric and Oceanic Technology*, Vol. 20, No. 8, 2003, pp. 1183–1195.
doi:10.1175/1520-0426(2003)020<1183:SFCEOA>2.0.CO;2

[15] Kopp, F., Rahm, S., and Smalikho, I., "Characterisation of Aircraft Wake Vortices by 2-μm Pulsed Doppler Lidar," *Journal of Atmospheric and Oceanic Technology*, Vol. 21, No. 2, 2004, pp. 194–206.
doi:10.1175/1520-0426(2004)021<0194:COAWVB>2.0.CO;2

[16] Kopp, F., Rahm, S., Smalikho, I., Harris, M., and Young, R. I., "Comparison of Wake-Vortex Parameters Measured by Pulsed and Continuous-Wave Lidars," *Journal of Aircraft*, Vol. 42, No. 4, 2005, pp. 916–923.
doi:10.2514/1.8177

[17] Rahm, S., Smalikho, I., and Kopp, F., "Characterization of Aircraft Wake Vortices by Airborne Coherent Doppler Lidar," *Journal of Aircraft*, Vol. 44, No. 3, 2007, pp. 799–805.
doi:10.2514/1.24401

[18] Rodenhiser, R. J., Durgin, W. W., and Johari, H., "Ultrasonic Method for Aircraft Wake Vortex Detection," *Journal of Aircraft*, Vol. 44, No. 3, 2007, pp. 726–732.
doi:10.2514/1.25060

[19] Dougherty, R. P., Wang, F. Y., Booth, E. R., Watts, M. E., Fenichel, N., and D'Errico, R. E., "Aircraft Wake Vortex Measurements at Denver International Airport," 10th AIAA/CEAS Aeroacoustics Conference, AIAA Paper 2004-2880, 2004.

[20] Burnham, D. C., and Hallock, J. N., "Measurement of Wake Vortices Interacting with the Ground," *Journal of Aircraft*, Vol. 42, No. 5, 2005, pp. 1179–1187.
doi:10.2514/1.10929

[21] Holzapfel, F., "Probabilistic Two-Phase Wake Vortex Decay and Transport Model," *Journal of Aircraft*, Vol. 40, No. 2, 2003, pp. 323–331.
doi:10.2514/2.3096

[22] Holzapfel, F., Gerz, T., and Baumann, R., "The Turbulent Decay of Trailing Vortex Pairs in Stably Stratified Environments," *Aerospace Science and Technology*, Vol. 5, No. 2, 2001, pp. 95–108.
doi:10.1016/S1270-9638(00)01090-7

[23] Proctor, F. H., and Switzer, G. F., "Numerical Simulation of Aircraft Trailing Vortices," Proceedings of the 9th Conference on Aviation, Range and Aerospace Meteorology, American Meteorology Society, Paper 7.12, Boston, Sept. 2000.

[24] Kantha, L. H., "Empirical model of the transport and decay of aircraft wake vortices," *Journal of Aircraft*, Vol. 35, No. 4, 1998, pp. 649–653.
doi:10.2514/2.2350

[25] Kantha, L. H., "A Simple Empirical Model of the Transport and Decay of Aircraft Wake Vortices Between Parallel Runways," *Journal of Aircraft*, Vol. 33, No. 4, 1996, pp. 752–760.
doi:10.2514/3.47011

[26] Kantha, L. H., and Clayson, C. A., *Small Scale Processes in Geophysical Flows*, Academic Press, San Diego, CA, 2000.

[27] Banakh, V. A., and Smalikho, I. N., "Estimation of the Turbulence Energy Dissipation Rate from the Pulsed Doppler Lidar Data," *Atmospheric and Oceanic Optics*, Vol. 10, No. 12, 1997, pp. 957–965.

[28] Banakh, V. A., Smalikho, I. N., Kopp, F., and Werner, C., "Measurements of Turbulent Energy Dissipation Rate with a CW Doppler Lidar in the Atmospheric Boundary Layer," *Journal of Atmospheric and Oceanic Technology*, Vol. 16, No. 8, Aug. 1999, pp. 1044–1061.
doi:10.1175/1520-0426(1999)016<1044:MOTEDR>2.0.CO;2

[29] Kopp, F., "Doppler Lidar Investigation of Wake Vortex Transport Between Closely Spaced Runways," *AIAA Journal*, Vol. 32, No. 4, 1994, pp. 805–810.
doi:10.2514/3.12057